NJC

ROYAL SOCIETY OF CHEMISTRY

PAPER

View Article Online
View Journal | View Issue

Cite this: *New J. Chem.*, 2025, **49**, 15723

Synthesis and coordination behaviour of a protic phosphinoferrocene amidine

Zdeněk Leitner, Ivana Císařová, Jana Kalbáčová Vejpravová and Petr Štěpnička *

A phosphinoferrocene amidine $Ph_2PfcN{=}CHNHiPr$ (**1**; fc = ferrocene-1,1′-diyl) has been synthesised and studied as a new P,N-hybrid donor in group 10 metal complexes. Thus, reactions with metal dichloride precursors produced tetrahedral and paramagnetic $[NiCl_2(\mathbf{1}\text{-}\kappa^2P,N)]$ and square-planar diamagnetic $[MCl_2(\mathbf{1}\text{-}\kappa^2P,N)]$ (M = Pd, Pt) and $[PdCl(Me)(\mathbf{1}\text{-}\kappa^2P,N)]$. The Pd(II) complex $[MCl_2(\mathbf{1}\text{-}\kappa^2P,N)]$ was converted to chloride-bridged dimers $[Pd_2(\mu\text{-}Cl)_2(\mathbf{1}\text{-}\kappa^2P,N)_2][BARF]_2$ and $[(\mu\text{-}Cl)\{PdCl(\mathbf{1}\text{-}\kappa^2P,N)\}_2][BF_4]$ (BARF = tetrakis(3,5-bis(trifluoromethyl)phenyl)borate) through reactions with halide scavengers. In solution, the former compound exists in equilibrium with monopalladium species featuring an Fe–Pd bond, $[PdCl(\mathbf{1}\text{-}\kappa^3Fe,P,N)][BARF]$. The interaction of **1** with $[Pd(MeCN)_4][BF_4]$ and triphenylphosphine produced analogous κ^3 complexes $[Pd(PPh_3)(\mathbf{1}\text{-}\kappa^3Fe,P,N)]X$ (X = BF_4 and, after anion exchange, also PF_6). Eventually, the compound family was expanded by a Pd(0) complex, $[Pd(\eta^2\text{-ma})(\mathbf{1}\text{-}\kappa^2P,N)]$, containing a π-coordinated maleic anhydride (ma). With the exception of the nonisolable $[PdCl(\mathbf{1}\text{-}\kappa^3Fe,P,N)][BARF]$, all reported compounds were fully characterised *via* a combination of elemental analysis, spectroscopic methods (ESI MS and NMR), and single-crystal X-ray diffraction analysis. Attempts to prepare complexes with a deprotonated terminal NH group failed. Nonetheless, the NH group plays the role of a structure-stabilising moiety, forming intramolecular NH···Cl hydrogen bonds with chloride ligands.

Received 15th July 2025,
Accepted 1st August 2025

DOI: 10.1039/d5nj02886h

rsc.li/njc

Introduction

Phosphines equipped with additional nitrogen donor groups are prototypical examples of hybrid and potentially hemilabile ligands[1] with widespread applications in coordination chemistry and transition metal catalysis.[2] Not surprisingly, ligands of this type were prepared with many central scaffolds, including ferrocene.[3] As representative examples of ferrocene P,N-donors[4] can serve functional derivatives of the widely investigated 1,1′-bis(diphenylphosphino)ferrocene (dppf),[5] such as phosphinoferrocene amines **A**,[6,7] pyridines **B**,[8] nitrile **C**,[9] Schiff bases **D**,[10] and oxazolines **E**[11] (Scheme 1). Of these compounds, nitrile **C** was used to prepare highly active, instant gold(I) catalysts $[Au_2(\mu(P,N)\text{-}\mathbf{C})_2]X_2$,[9b] compounds **D** (with varied phosphine and imine substituents) were applied as ligands in Pd-catalysed Suzuki–Miyaura cross-coupling[10a] and Ni-catalysed ethylene oligomerization,[10b–e] while phosphinoxazolines were utilised as versatile chiral ligands for asymmetric catalysis.[12]

Recently, we reported the synthesis of phosphinoferrocene guanidines **F**,[13] which also fall into this ligand class. In contrast to their guanidinium counterparts,[14] the guanidine moiety in type **F** compounds readily coordinates soft Pd(II) and Pt(II) ions,

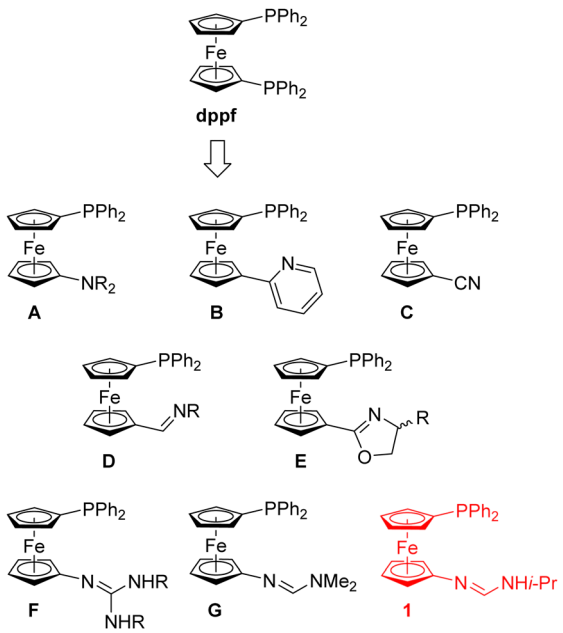

Scheme 1 Dppf and its formal analogues having one phosphine moiety replaced with an N-donor group (R = various alkyl and aryl groups; for **F**, R = isopropyl, cyclohexyl, and 2,6-xylyl; in addition to the presented compounds, several dialkylphosphino derivatives have also been reported) and the presently reported ligand **1**.

Department of Inorganic Chemistry, Faculty of Science, Charles University, Hlavova 2030, 128 00 Prague, Czech Republic. E-mail: stepnic@natur.cuni.cz

giving rise to P,N-chelate complexes, which can be further transformed to κ^3Fe,P,N complexes.[13a] In a subsequent study, we focused on the related phosphinoferrocene amidine **G**, which formally lacks one NR_2 group.[15,16]

As a continuation of our research, we now describe the synthesis of the analogous protic phosphinoferrocene amidine **1**. This compound was explored as a ligand for group 10 metal complexes with an emphasis on accessible coordination modes and their mutual interconversion. Particular attention was given to the preparation of the κ^3Fe,P,N complexes featuring the Fe → Pd dative bond unique to ferrocene-based ligands,[17] and species with a deprotonated terminal NH group.

Results and discussion

Amidine **1** was obtained *via* a one-pot procedure involving acid-catalysed condensation of 1′-(diphenylphosphino)-1-aminoferrocene (**2**) with triethyl orthoformate and subsequent reaction of the nonisolated formimidate intermediate with isopropylamine (Scheme 2).[18] After chromatographic purification and crystallisation, the compound was isolated as an orange crystalline solid in 43% yield.

Amidine **1** was characterised by multinuclear NMR spectroscopy, electrospray ionisation (ESI) mass spectrometry, and elemental analysis. In addition, the solid-state structure was determined using single-crystal X-ray diffraction analysis. The NMR spectra contained characteristic signals of the phosphinoferrocenyl substituent, including the $^{31}P\{^1H\}$ NMR resonance at δ_P −18.3 (in DMSO-d_6; *cf.* $\delta_P \approx -16$ for (diphenylphosphino)ferrocene in $CDCl_3$[19]). The presence of the amidine fragment was confirmed by the signals of the imine CH (δ_H 7.70, δ_C 150.51) and the terminal isopropyl group.

The molecule of **1** (Fig. 1) contains an unperturbed ferrocene moiety (Fe–C 2.039(1)–2.079(1) Å, tilt angle: 1.96(7)°), and the substituents assume an approximately 1,2′[20] eclipsed conformation (τ = −80.26(8)°).[21] The amidine unit {N1,C11,N2} is twisted by 38.9(1)° from the plane of the bonding cyclopentadienyl ring C(1–5) and has a regular geometry (C11–N1 1.282(2), C11–N2 1.348(2) Å; N1–C11–N2 122.6(1)°)[15,22] and an (*E*) configuration at the CH=N bond (N1–C11–N2–C24 = −7.8(2)°).

The coordination behaviour of **1** was probed *via* reactions with MCl_2 precursors, where M is a group 10 metal ion. The reactions with [$NiCl_2$(dme)], [$PdCl_2(MeCN)_2$] and [$PtdCl_2$(cod)] (dme = 1,2-dimethoxyethane, cod = cycloocta-1,5-diene) in suitable solvents proceeded smoothly to yield chelate complexes of the type [MCl_2(**1**-κ^2P,N)] (**3–5**; Scheme 3).

Nickel(II) complex **3** was isolated as a deep-coloured (seemingly black) crystalline solid that readily decomposed after dissolution in standard (wet) solvents and did not dissolve in anhydrous organic solvents. The compound was paramagnetic, which, together with other analytical data, indicated that it was a tetrahedral complex of the [$NiCl_2L_2$] type. Subsequent measurements revealed that the molar magnetic susceptibility (χ_m) of **3** is independent of the applied magnetic field (1, 2, or 4 T over the 3–300 K temperature range; see Fig. 2 and the SI). The collected data were evaluated *via* the Curie–Weiss law:

$$\chi_m = \frac{N_A \mu_{eff}^2}{3k_B} \frac{1}{T - \theta_p} = \frac{C}{T - \theta_p}$$

where N_A and k_B represent the Avogadro constant and Boltzmann constant, respectively; θ_p is the Curie paramagnetic temperature; μ_{eff} is the effective magnetic moment; and C represents the Curie constant. Fitting of the experimental values ($1/\chi_m$ *vs.* T) yielded C = 1.4(2) × 10^{-5} m^3 K^{-1} mol^{-1} and θ_p = −5(1) K (Fig. 2). The estimated effective magnetic moment, μ_{eff} = 3.01(2)μ_B, was higher than the spin-only value expected for two unpaired electrons (n = 2), $\mu_{eff}/\mu_B = [n(n+1)]^{1/2} \approx 2.83$,[23] but aligned well with the values reported for Ni^{2+} phosphine complexes with tetrahedral coordination.[24]

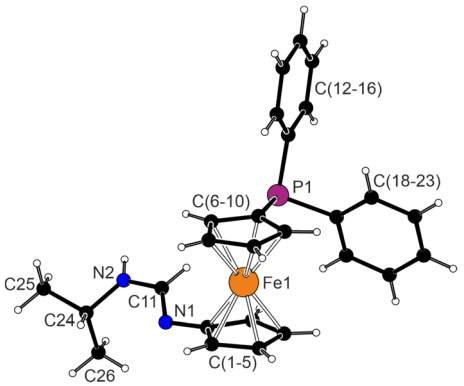

Fig. 1 Molecular structure of **1** (for a displacement ellipsoid plot, see the SI).

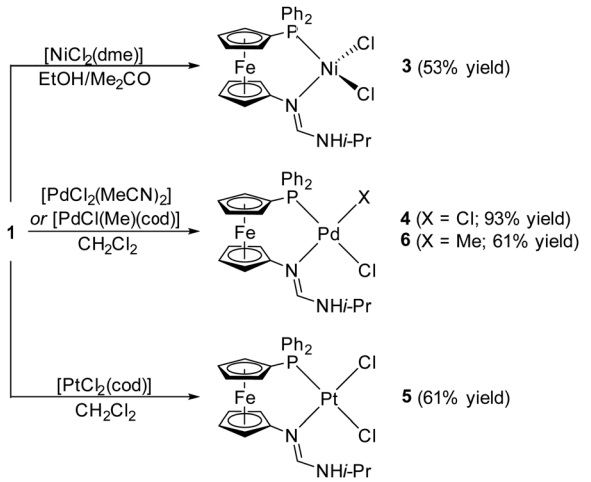

Scheme 3 Synthesis of group 10 metal complexes **3–5** (cod = cycloocta-1,5-diene, dme = 1,2-dimethoxyethane).

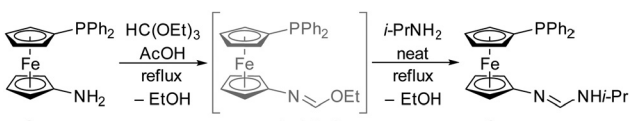

Scheme 2 Synthesis of phosphinoferrocene amidinate **1**.

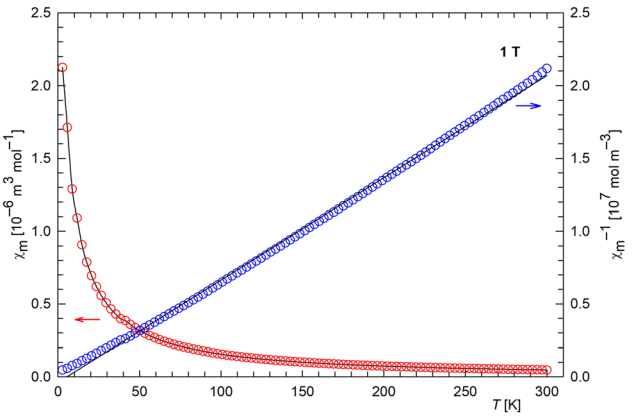

Fig. 2 Temperature dependence of the molar susceptibility (χ_m; red) and inverse molar susceptibility (χ_m^{-1}; blue) of compound **3** under a 1 T magnetic field (for additional diagrams, see the SI).

X-ray diffraction analysis of single crystals obtained by reactive diffusion of the ligand in acetone into an ethanolic solution of [$NiCl_2$(dme)] (see Scheme 3) ultimately confirmed the tetrahedral arrangement around the Ni(II) ion (Fig. 3). The ferrocene cyclopentadienyls in complex **3** are practically parallel (tilt angle 2.6(1)°) and eclipsed (τ = −7.0(1)°), forming a P,N-donor pocket for the $NiCl_2$ moiety located on the side of the ferrocene unit. The amidine unit {N1,C11,N2} is twisted by 59.7(2)° from the plane of ring C(1–5).

The Ni-donor distances are similar to those in [$NiCl_2$(dppf-κ^{2}P,P′)][25] and the amidine complex [$NiCl_2$(TolN=CHNHTol-κN)$_2$] (Tol = 4-tolyl).[26] However, the coordination environment is angularly distorted, as indicated by the τ_4 index of 0.85 (ideal tetrahedral and planar coordination would yield τ_4 = 1 and 0, respectively).[27] Among the interligand angles, the P1–Ni1–N1 and P1–Ni1–Cl1 angles are the narrowest (101° and 102°), and the Cl1–Ni1–Cl2 and N1–Ni1–Cl2 angles are the widest (122° and 118°).[28]

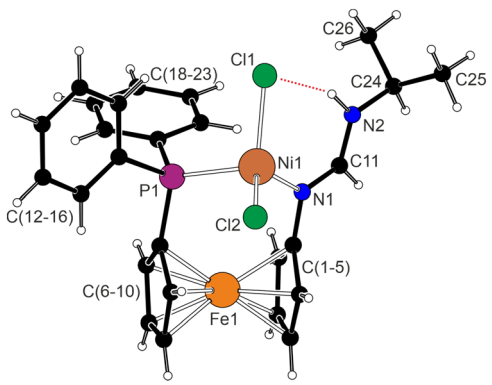

Fig. 3 Molecular structure of **3** (for a displacement ellipsoid plot, see the SI). The intramolecular N2–H2N···Cl1 hydrogen bond is shown as a red dotted line (N2···Cl1 = 3.164(2) Å). Selected distances and angles (in Å and deg): Ni1–P1 2.2867(7), Ni1–N1 1.982(2), Ni1–Cl1 2.2612(6), Ni1–Cl2 2.2155(5), P1–Ni1–N1 100.56(5), P1–N1–Cl1 101.57(2), P1–Ni1–Cl2 104.30(3), N1–Ni1–Cl1 107.23(5), N1–Ni1–Cl2 117.99(5), Cl1–N1–Cl2 121.53(2); N1–C11 1.313(2), N2–C11 1.313(3), and N1–C11–N2 124.7(2).

Conversely, Pd(II) and Pt(II) complexes **4** and **5** were square planar diamagnetic, as expected for heavy d^8 metal ions. The compounds were characterised by NMR spectroscopy, ESI MS, and elemental analysis. Although the $^{31}P\{^1H\}$ NMR spectrum of **4** recorded at 25 °C exhibited a sharp singlet at δ_P = 28.8 (in 1,2-$C_2D_4Cl_2$), the ^1H NMR spectrum showed broad signals, indicating slow structural dynamics. After cooling to −25 °C, the ^1H NMR signals sharpened and resolved into defined multiplets. Thus, seven signals (6 × 1 H plus 1 × 2 H) were identified for the ferrocene CH groups, indicating a fixed geometry that renders these groups diastereotopic. An analogous pattern was observed in the low-temperature $^{13}C\{^1H\}$ NMR spectrum (eight CH signals and two C^{ipso} signals for the ferrocene unit). The signals due to the CH*Me*$_2$ groups and the PPh_2 moiety were similarly affected.

In contrast, the ^1H NMR spectrum of **5** was similar and exhibited sharp signals even at 25 °C, indicating a fixed molecular geometry at this temperature. The $^{31}P\{^1H\}$ NMR signal was observed at δ_P 5.3 as a singlet flanked by satellites due to the ^{195}Pt isotopomer ($I = \frac{1}{2}$, $^1J_{PtP}$ = 2042 Hz).

The compounds crystallised as solvates **4**·CH_2Cl_2 and **5**·CH_2Cl_2 with two complex molecules per asymmetric unit and very similar (practically isostructural) overall structures. The complex molecules differ only in conformation, mainly in the rotation of the phenyl rings and position of the coordination plane relative to the ferrocene ligand. A view of molecule **1** in the structure of **4**·CH_2Cl_2 is shown in Fig. 4; additional structure diagrams are available in the SI.

The geometric parameters listed in Table 1 highlight the general similarity of the [MCl_2(**1**-κ^{2}P,N)] molecules (M = Pd and Pt). The central atoms in the four molecules have square planar coordination with *cis*-interligand angles near 90° ($\tau_4 \leq 0.10$ in all cases). The Pd-donor distances compare well with the data reported for the related phosphinoguanidine complexes, [MCl_2(Ph_2PfcN=C(NHi-Pr)$_2$-κ^{2}P,N)].[13] Owing to the strong *trans* influence of the phosphine moiety,[29] the M–Cl bonds located *trans* to phosphorus are consistently longer than those *trans* to nitrogen. The coordination planes are located on the side of the ferrocene moiety, whose cyclopentadienyl rings are eclipsed to facilitate chelate coordination.

In the following experiments, we focused on palladium complexes in greater detail. Thus, the reaction of **1** with

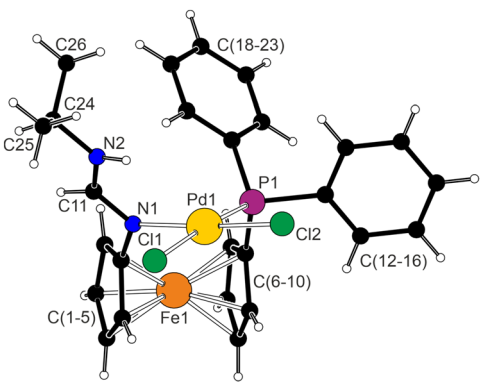

Fig. 4 View of complex molecule 1 in the structure **4**·CH_2Cl_2.

Table 1 Selected geometric parameters for **4**·CH_2Cl_2 and **5**·CH_2Cl_2 (in Å and deg)

	4·CH_2Cl_2 (M = Pd)		**5**·CH_2Cl_2 (M = Pt)	
Parameter[a]	Molecule 1	Molecule 2	Molecule 1	Molecule 2
M1–P1	2.2584(7)	2.2688(7)	2.2323(6)	2.2408(6)
M1–N1	2.044(2)	2.036(2)	2.036(2)	2.032(2)
M1–Cl1	2.3571(8)	2.3703(7)	2.3623(6)	2.3696(5)
M1–Cl2	2.2931(7)	2.2878(7)	2.3039(6)	2.2967(6)
P1–M1–N1	91.76(6)	90.87(6)	91.92(5)	91.59(2)
P1–M1–Cl2	90.43(3)	91.96(3)	92.01(2)	93.62(2)
N1–M1–Cl1	87.30(6)	86.51(6)	86.54(5)	85.42(5)
Cl1–M1–Cl2	90.91(2)	90.90(2)	89.70(2)	89.25(2)
τ	−8.7(2)	3.1(2)	−6.9(2)	2.0(2)
Tilt	3.2(1)	3.0(2)	3.7(1)	3.2(1)
C11–N1	1.307(3)	1.298(3)	1.308(3)	1.304(3)
C11–N2	1.317(3)	1.318(3)	1.319(3)	1.313(3)
N1–C11–N2	123.4(2)	122.9(2)	124.0(2)	123.5(2)
ω	57.7(3)	45.2(3)	56.1(3)	47.8(2)

[a] τ represents the torsion angle C1–Cg1–Cg2–Cg, where Cg1 and Cg2 stand for the centroids of the cyclopentadienyl rings C(1–5) and C(6–10), respectively. Tilt is the dihedral angle of the least-squares cyclopentadienyl planes, and ω is the angle between the amidine unit {N1, C11, N2} and the parent cyclopentadienyl ring C(1–5). Note: the atomic labelling of all the molecules is strictly analogous.

$[PdCl_2(MeCN)_2]$ was also performed at a 1 : 2 Pd : **1** ratio to prepare a "phosphine" complex $[PdCl_2(\mathbf{1}\text{-}\kappa P)_2]$. Surprisingly, this reaction resulted in a mixture showing complicated NMR spectra (δ_P −15, 15, and 30; this probably corresponds to a mixture of free ligand, a possible bisphosphine complex and **4**, respectively). Attempts to isolate any of the products by crystallisation were unsuccessful.

Conversely, the reaction of [PdCl(Me)(cod)] with an equimolar amount of **1** proceeded cleanly to yield complex **6** as a single isomer (Scheme 3). The presence of the Pd-bound methyl group was confirmed by the NMR signals at δ_H 0.33 (d, J_{PH} = 4.2 Hz) and δ_C 3.08 (d, J_{PC} = 4 Hz). The $^{31}P\{^1H\}$ NMR resonance was detected at δ_P 32.6 (in CD_2Cl_2).

Structure determination (Fig. 5) revealed that complex **6** results as a *trans*-P,Cl isomer, as dictated by the "antisymbiosis" of the strongly *trans*-influencing ligands (P and CH_3) that tend to avoid mutually opposite positions.[30] Otherwise, the molecular structure does not significantly differ from that of complexes **4** and **5** (*vide supra*), with the exception that the *trans* influence of the methyl ligand results in elongation of the Pd1–N1 bond (by ≈0.11 Å compared with **4**). The interligand angles in **6** fall in the 88–92° range (τ_4 = 0.07). The ferrocene unit is eclipsed (τ = 2.0(2)°) and negligibly tilted (3.7(1)°), and the amidine unit is twisted 43.0(2)° from the plane of ring C(1–5).

Further experiments (Scheme 4) aimed at the preparation of Pd(II) complexes with an Fe–Pd dative bond.[17] In particular, complex **4** was treated with Na[BARF] in anhydrous dichloromethane (**4** : Na[BARF] = 1 : 1, BARF = tetrakis(3,5-bis(trifluoromethyl)phenyl)borate) to eliminate one Pd-bound chloride. After mixing, the reaction mixture turned from red to green, and subsequent crystallisation by hexane diffusion afforded deep green crystals of the chloride-bridged dimer $[Pd_2(\mu\text{-}Cl)_2(\mathbf{1}\text{-}\kappa^2P,N)_2][BARF]_2$ (**7**). When it was dissolved in CD_2Cl_2, complex **7** produced a red-brown dichroic solution. This colour change

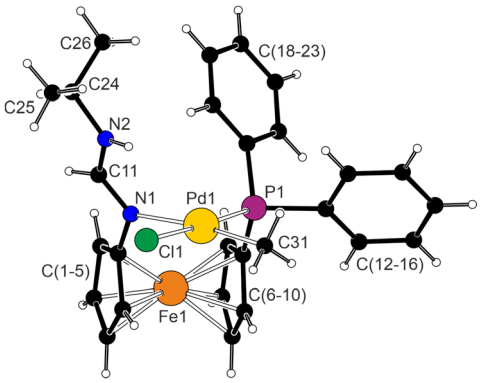

Fig. 5 Molecular structure of **6**. Selected distances and angles (in Å and deg): Pd1–P1 2.2342(5), Pd1–N1 2.151(2), Pd1–Cl1 2.3731(6), Pd1–C31 2.032(2), P1–Pd1–N1 92.13(5), P1–Pd1–C31 91.33(7), N1–Pd1–Cl1 88.82(5), Cl1–Pd1–C31 88.06(7), N1–C11 1.291(3), N2–C11 1.325(3), and N1–C11–N2 121.9(2).

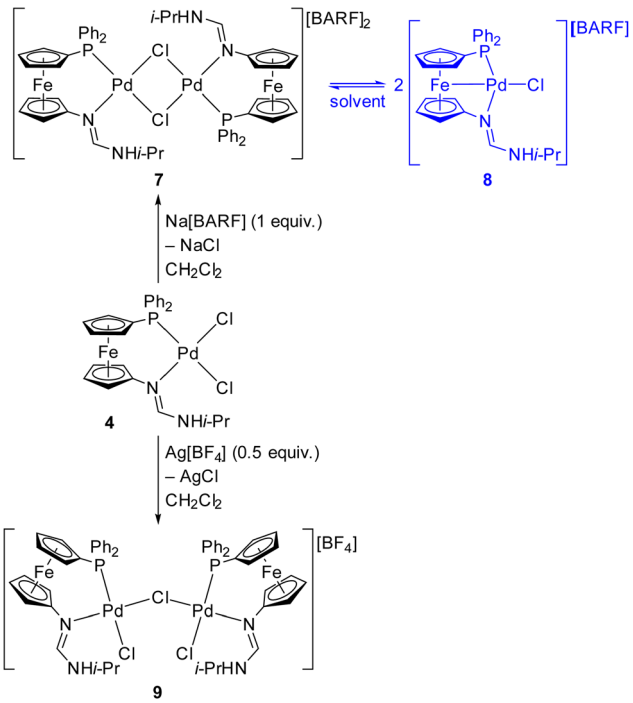

Scheme 4 Synthesis of chloride-bridged complexes **7** and **9** and the equilibrium between complexes **7** and **8** ($[BARF]^-$ = $[(3,5\text{-}(CF_3)_2C_6H_3)_4B]^-$).

and the $^{31}P\{^1H\}$ NMR signal at δ_P −9.5 indicated dissociation of the dimer into monopalladium species $[PdCl(\mathbf{1}\text{-}\kappa^3Fe,P,N)][BARF]$ (**8**) featuring an Fe → Pd interaction. Further support was provided by the ^1H NMR spectrum showing one set of resonances due to the ferrocene unit, which were markedly differentiated into two separate groups typical for complexes with Fe–Pd interactions and tilted ferrocene units (high-field signals at δ_H 3.34 and 3.55; low-field signals at δ_H 5.49 and 5.78).

In acetone-d_6, the $^{31}P\{^1H\}$ NMR signal shifted to δ_P −7.6, and additional broad resonances were observed at approximately

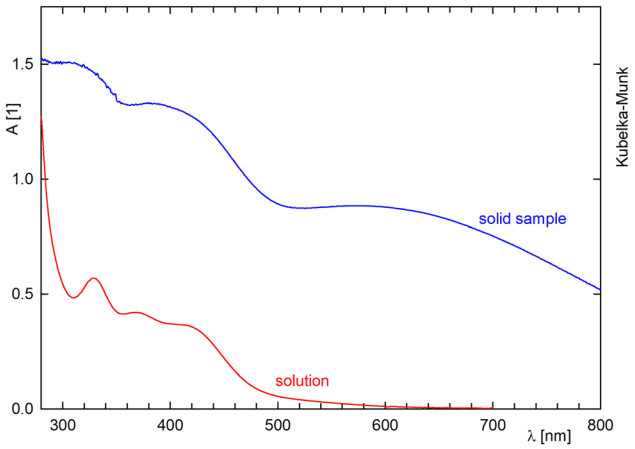

Fig. 6 UV-vis spectra of **7** recorded in dichloromethane solution (c = 0.048 mM, optical path 1 cm; red line) and as a solid (diffuse reflectance mode; blue line).

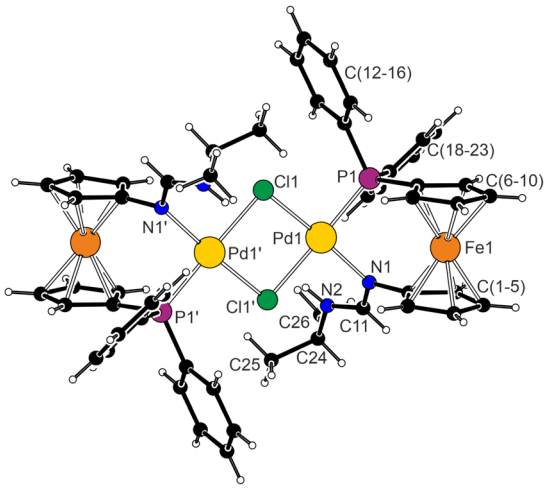

Fig. 7 View of the complex cation in the structure of **7**·CH_2Cl_2 (for a complete diagram, see the SI). Selected distances and angles (in Å and deg): Pd1–P1 2.2449(6), Pd1–N1 2.033(2), Pd1–Cl1 2.3152(6), Pd1–Cl1′ 2.4097(7), P1–Pd1–N1 91.03(5), P1–Pd1–Cl1 92.32(2), N1–Pd1–Cl1′ 90.28(5), Cl1–Pd1–Cl1′ 86.36(2), N1–C11 1.305(2), N2–C11 1.318(3), and N1–C11–N2 124.9(2). The prime labelled atoms are generated by the inversion operation.

δ_P 36.3, 38.2 and 39.3, attributable to the stereoisomers of dimer **7**.[13b,15] Overall, the removal of one chloride ligand from **4** resulted in the formation of dimeric product **7**, which selectively crystallises due to its lower solubility. In solution, however, complex **7** exists in equilibrium with monopalladium species **8**, whose relative amount depends on the solvent. This finding was indeed reflected in the UV-vis spectra (Fig. 6). The spectrum of solid **7** exhibited absorption bands at approximately 350–450 nm and a broad absorption at approximately 600 nm, which render dimer **7** emerald green. In contrast, the spectrum recorded in a dichloromethane solution showed a band at 328 nm and, mainly, a broad and composite absorption in the 350–500 nm region, which was responsible for the observed burgundy red colour attributed to **8**.

When the amount of the halide scavenger, now $Ag[BF_4]$, was reduced to a half molar equivalent relative to **4**, the reaction yielded another chloride-bridged dimer, $[(\mu\text{-Cl})\{Pd(\mathbf{1}\text{-}\kappa^2P,N)\}_2][BF_4]$ (**9** in Scheme 4). Apparently, halide removal generated a coordinatively unsaturated species that interacted with the remaining **4** to produce complex **9** under saturation of the coordination sphere. In a 1,2-$C_2D_4Cl_4$ solution at room temperature, the compound presented two $^{31}P\{^1H\}$ NMR signals, attributable to two isomers (presumably conformers; δ_P 31.2 and 32.9). A variable-temperature ^1H NMR study revealed that the species were in dynamic exchange, which was expectedly slower at a low temperature (see the SI).

Compounds **7**·CH_2Cl_2 and **9**·CH_2Cl_2 were authenticated structurally *via* single-crystal X-ray diffraction analysis. The former compound crystallises with imposed inversion symmetry (Fig. 7), which renders only half of the complex cation structurally independent and makes the $\{Pd_2P_2N_2Cl_4\}$ central part ideally planar and *trans*-configured [in principle, the compound can form four isomers differing by the mutual orientation of chelating ligands (*cis*/*trans*) and the ferrocene units (*syn*/*anti*); see the NMR spectra above].[13b,15]

The donor atoms in **7**·CH_2Cl_2 create a planar coordination environment for Pd(II) (τ_4 = 0.03); the associated interligand angles are 86–92° (the Cl1–Pd1–Cl1′ angle is the smallest). The Pd-donor distances are similar to those in parent complex **4** (*vide supra*). Even in this case, however, a lengthening of the Pd–Cl bond *trans* to phosphorus is observed. The ferrocene unit has an eclipsed conformation and parallel cyclopentadienyl rings (τ = −5.02(2), tilt angle 2.8(1)°) and is located on one side, while the phosphine and amidine substituents are located on the other side relative to the coordination plane. These positions are swapped for the other Pd atom due to external symmetry. The amidine plane is twisted 57.7(3)° from the plane of ring C(1–5).

The complex cation of **9**·CH_2Cl_2 (Fig. 8) consists of two mutually twisted $\{PdPNCl_2\}$ planes connected by a bridging chloride ligand (interplanar angle: 64.80(3)°; Pd1–Cl2–Pd2 = 98.98(2)°). The τ_4 indices of 0.03 (Pd1) and 0.15 (Pd2) indicate a larger angular distortion for Pd2. This observation corresponds with greater tilting (7.8(1)°) and a more open conformation (τ = −28.0(2)°) of ferrocene unit 1 (Fe1) than of ferrocene unit 2, which adopts a stiffer 1,1′ conformation[31] (Fe2; tilting 3.7(1)°, τ = −1.4(2)°). A corresponding difference is observed in the orientation of the amidine planes relative to their parent cyclopentadienyl rings, as shown by the tilt angles of 15.7(3)° (N1, C11, and N2) and 40.3(2)° (N3, C41, and N4; this plane diverts more from a coplanar arrangement for steric reasons). The structure is stabilised by intramolecular N2–H2N···Cl3 (N2···Cl3 = 3.266(2) Å) and N4–H4N···Cl1 (N4···Cl1 = 3.310(2) Å) hydrogen bonds.

To entirely eliminate the influence of strongly coordinating chloride ligand(s), we next employed the nitrile complex[32] $[Pd(MeCN)_4][BF_4]_2$ as the Pd(II) source. After it was mixed with 1 molar equivalent of ligand **1** and triphenylphosphine,[33] this precursor smoothly transformed to the κ^3Fe,Pd,N complex

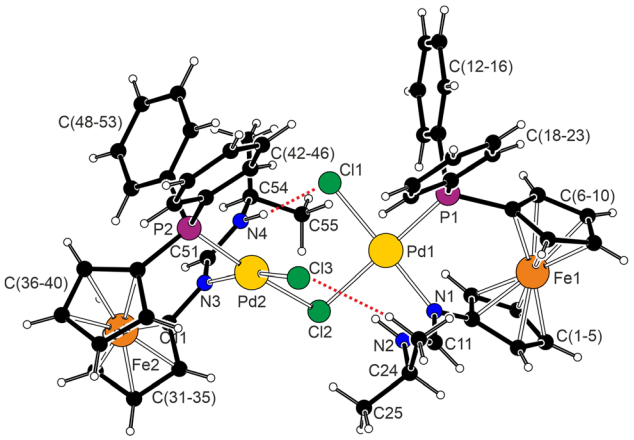

Fig. 8 View of the complex cation in the structure of **9**·CH_2Cl_2 (for a complete diagram, see the SI). Selected distances and angles (in Å and deg): Pd–P1 2.2515(7), Pd1–N1 2.038(2), Pd1–Cl1 2.3094(6), Pd1–Cl2 2.4072(8), P1–Pd1–N1 93.27(5), P1–Pd1–Cl1 86.85(2), N1–Pd1–Cl2 87.12(5), Cl1–Pd1–Cl2 92.78(3); Pd2–P2 2.2340(7), Pd2–N2 2.040(2), Pd2–Cl3 2.3086(8), Pd2–Cl2 2.4137(6), P2–Pd2–N3 87.96(5), P2–Pd2–Cl3 93.29(2), N3–Pd2–Cl2 88.16(5), and Cl2–Pd–Cl3 92.07(3). The N–H···Cl interactions are indicated by red dotted lines.

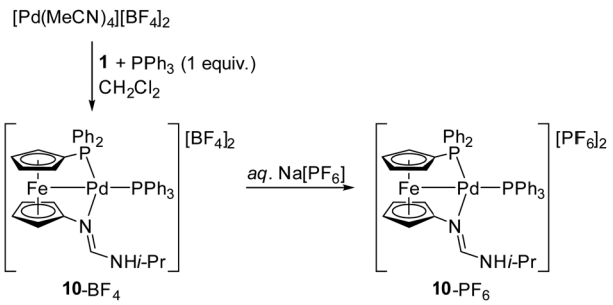

Scheme 5 Preparation of κ^3Fe,Pd,N complexes **10**-BF_4 and **10**-PF_6.

10-BF_4 (Scheme 5), which was isolated as a deep red crystalline solid in 73% yield. Subsequent ion exchange with aqueous Na[PF_6] produced **10**-PF_6 (48% yield after crystallisation).

Complexes **10**-BF_4 and **10**-PF_6 were characterised by NMR spectroscopy, ESI MS and elemental analysis. In addition, the crystal structures were determined by X-ray diffraction analysis. Their $^{31}P\{^1H\}$ NMR spectra revealed a pair of signals at approximately δ_P −6 (PPh_2) and 31 (PPh_3), split into doublets with a relatively small coupling constant ($^2J_{PP} \approx 25$ Hz) corresponding to the *cis*-arrangement of the phosphine donor groups (an additional signal of PF_6^- was observed for **10**-PF_6). The ^1H and $^{13}C\{^1H\}$ NMR spectra were consistent with the proposed structure, showing signals due to the ferrocene CH groups characteristically divided into two anisochronic groups in both spectra (δ_H 3.5–4.1 and 5.7–6.0; δ_C 68–73 and 82–88).

The molecular structure of **10**-PF_6 is displayed in Fig. 9. The relevant structural parameters for this compound and for **10**-BF_4, which crystallises with three independent molecules, are presented in Table 2.

The cations in the crystal structures of **10**-BF_4 and **10**-PF_6 differ practically insignificantly. They exert the typical opening

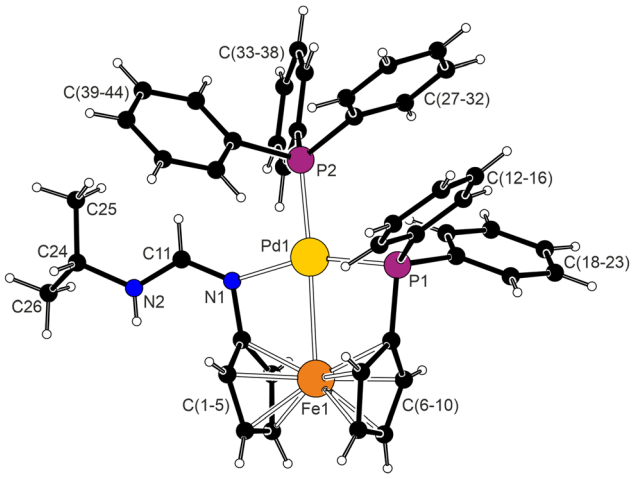

Fig. 9 View of the complex cation in the structure of **10**-PF_6 (for a complete diagram and the structure of **10**-BF_4, see the SI). Only one orientation of the disordered isopropyl groups is shown for clarity.

Table 2 Selected distance and angles data for **10**-BF_4 and **10**-PF_6 (in Å and deg)

	10-BF_4			
Parameter[a]	Mol 1	Mol 2	Mol 3	**10**-PF_6
Pd1–Fe1	2.8392(6)	2.8625(6)	2.8570(6)	2.8524(4)
Pd1–P1	2.2090(6)	2.2088(6)	2.2104(6)	2.2105(4)
Pd1–P2	2.2762(7)	2.2791(7)	2.2806(7)	2.2840(4)
Pd1–N1	2.035(2)	2.037(2)	2.033(2)	2.038(1)
Fe1–Pd1–P1	82.69(2)	82.10(2)	82.34(2)	80.90(1)
Fe1–Pd1–N1	77.58(6)	77.70(6)	77.36(6)	78.51(4)
P2–Pd1–P1	101.54(3)	100.40(3)	100.86(3)	100.43(2)
P2–Pd1–N1	97.69(6)	99.43(6)	99.11(6)	100.22(4)
Tilt	21.4(1)	21.1(1)	21.4(1)	22.62(9)
τ	−16.7(2)	−4.4(2)	9.2(2)	−5.9(1)
C11–N1	1.299(3)	1.297(3)	1.291(3)	1.301(2)
C11–N2	1.309(3)	1.320(4)	1.318(4)	1.313(2)
N1–C11–N2	126.7(2)	125.6(3)	126.4(3)	126.5(1)
ω	74.7(3)	83.5(1)	86.7(3)	73.7(2)

[a] τ is the torsion angle C1–Cg1–Cg2–Cg, where Cg1 and Cg2 denote the centroids of the cyclopentadienyl rings C(1–5) and C(6–10), respectively. Tilt is the dihedral angle of the least-squares cyclopentadienyl planes, and ω is the angle between the amidine unit {N1, C11, and N2} and the cyclopentadienyl ring C(1–5).

of the ferrocene unit in a tweezer-like manner, which enables the Fe → Pd interaction. This opening is manifested by varying the Fe–C distances (2.05–2.13 Å) and tilt angles (21–22°) and is further associated with the closing of the inner (Fe1–Pd1–P1–N2; ≈80°) and opening of the outer (P2–Pd1–P1–N1; ≈100°) "interligand" angles. Correspondingly, the ligand bite angle P1–Pd1–N1 increases to approximately 160°. The coordination environment of the Pd(II) ion thus remains planar but is angularly distorted. The amidine plane is diverted from the ferrocene moiety. However, as the PPh_3 ligand increases steric congestion, the ω angles (Table 2) are larger than those in the chelate complexes discussed above. The Fe–Pd distances are approximately 2.85 Å and do not vary appreciably among the individual molecules. This distance is similar to that in

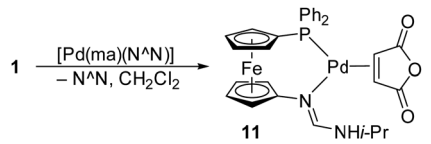

Scheme 6 Synthesis of Pd(0) complex **11**.

$[Pd(Ph_2PfcNMe_2\text{-}\kappa^3Fe,P,N)(PPh_3)][BF_4]_2$ (2.829(2) Å) but longer than that in the chloride complexes $[PdCl(L\text{-}\kappa^3Fe,P,N)][SbF_6]_2$ (L = $Ph_2PfcNMe_2$: 2.738(2) Å,[34] and $Ph_2PfcN{=}C(NHiPr)_2$: 2.7590(5) Å;[13a] fc = ferrocene-1,1′-diyl) due to the large *trans* influence of the monodentate phosphine.

Notably, repeated attempts to prepare a Pd(II) complex containing anionic phosphinoamidinate failed. Deprotonation of **4** with $MN(SiMe_3)_2$ (M = Li or K), NaOMe, TlOMe, or *n*-butyllithium resulted in only intractable mixtures and palladium black. This behaviour differentiates amidine ligand **1** from the related guanidine **F** (Scheme 1),[13] which provides this P,N,N-guanidinate complex.

The series of compounds were eventually expanded by a Pd(0) complex featuring an auxiliary η^2-olefin ligand, [Pd(**1**-κ^2P,N)(ma)] (**11**). This complex was obtained by replacing[35] the diimine ligand (N^N) in [Pd(ma)(N^N)] (ma = maleic anhydride, N^N = *N*,*N*′-di-*t*-butylethane-1,2-diimine) with one molar equivalent of **1** (Scheme 6) and was isolated as an air stable, orange crystalline solid in good yield (76%). However, after it crystallised, it was only very poorly soluble, which made any solution NMR analysis impossible. Therefore, the characterisation was based on mass spectra and elemental analysis and was later unambiguously supported by structure determination (Fig. 10).

Compound **11** is a pseudotrigonal Pd(II) complex with P,N-chelating **1** and η^2-bound maleic anhydride as the ligands.[36] The alkene is coordinated in a side-on fashion so that the C_4O ring is tilted by 73.21(6)° relative to the {Pd1, P1, N1} plane, consistently with the Dewar–Chatt–Duncanson bonding model.[37] Compared with the free anhydride, the C31═C32 bond (1.428(2) Å) is elongated by approximately 0.1 Å.[38]

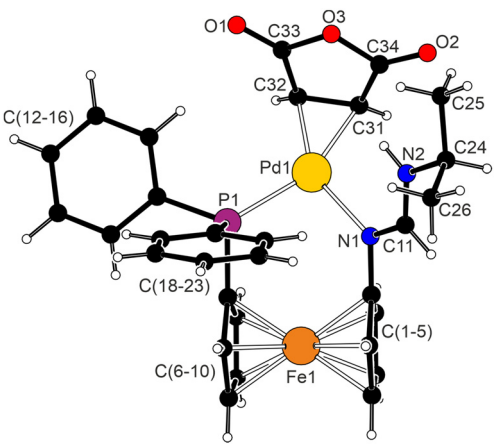

Fig. 10 Molecular structure of **11** (for a displacement ellipsoid plot, see the SI).

Due to unlike *trans* influence[29] and steric properties of the P- and N-donor groups, the ma ligand binds somewhat asymmetrically (Pd1–C31 2.118(1) Å, Pd1–C32 2.080(1) Å). The ferrocene unit has an eclipsed conformation (τ = 0.51(8)°) and is tilted by 4.05(8)°. Notably, the Pd1–P1 (2.3173(5) Å) and Pd1–N1 (2.151(1) Å) bonds are longer than those in **3**, likely due to the strong *trans* influence of the alkene ligand (Cl < η^2-alkene); the bite angle P1–Pd1–N1 is 95.50(3)°.

Conclusions

We have reported the synthesis of the new protic phosphinoferrocene amidine **1** and explored its coordination behaviour in complexes with group 10 metals. The collected data indicate that compound **1** strongly favours the formation of P,N-chelate complexes. This can be explained by the relatively rigid structure of this ligand as mutual positioning of the ferrocene-bound P and N donor atoms can be changed only through rotation of the cyclopentadienyl rings,[39] which tend to retain a parallel arrangement with an interplanar separation of approximately 3.3 Å. Tilting of the ferrocene unit increases the overall energy,[40] which must be compensated by other factors (*e.g.*, by formation of Fe → Pd dative interactions in κ^3Fe,P,N complexes). Attempts to prepare (isolable) complexes with a deprotonated NH group failed. However, the uncoordinated NH moiety seems to play a role in stabilisation of the formed structures *via* NH···X hydrogen bonds, either intramolecular (for chloride complexes, X = Cl) or intermolecular (for **10**-BF_4 and **10**-PF_6, X = F).

Experimental

Materials and methods

The syntheses were performed under a nitrogen atmosphere using standard Schlenk techniques. 1′-(Diphenylphosphino)-1-aminoferrocene (**2**),[6c] [PdClMe(cod)] (cod = cycloocta-1,5-diene),[41] and [Pd(ma)(N^N)] (ma = maleic anhydride, N^N – *N*,*N*′-di-*t*-butylethane-1,2-diimine)[35a,b] were prepared according to procedures reported in the literature. Other chemicals were obtained from commercial sources (Sigma-Aldrich and TCI) and used as received. The acetone was dried over potassium carbonate and distilled. Anhydrous dichloromethane was obtained from a PureSolv MD5 solvent purification system (Innovative Technology, USA). Isopropylamine (reagent grade from Sigma-Aldrich) was used as received. The solvents utilised for chromatography and crystallisations were used without additional purification (Lach-Ner, p.a. grade).

The NMR spectra were recorded at 25 °C on a Varian Unity Inova 400, Bruker Avance III 400, or Varian NMR System 300 spectrometer. Chemical shifts (δ in ppm) are expressed relative to internal $SiMe_4$ (^{1}H and ^{13}C), external 85% H_3PO_4 (^{31}P), and external neat $CFCl_3$ (^{19}F). Electrospray ionisation mass spectra were acquired using a Compact QTOF-MS spectrometer (Bruker Daltonics).

The magnetic properties were measured using a magnetic property measurement system equipped with a Superconducting Quantum Interference Device (MPMS 7XL, Quantum Design, USA). The sample was placed in a gelatine capsule and inserted into a low-background measurement straw provided by the manufacturer. The sample was cooled down to 3 K in the negligible remanent field of the superconducting magnet and the data were collected during a heating sweep at 1 K min^{-1} under static magnetic fields of 1, 2, and 4 T. For further evaluation, the data were converted to molar units.

Elemental analyses were performed on a PE 2400 Series II CHNS/O Elemental Analyser (PerkinElmer). The amount of residual solvent was verified by NMR analysis. Details of the structure determined by single-crystal X-ray diffraction analysis are available in the SI.

Syntheses

Synthesis of amidine 1. An oven-dried, nitrogen-flushed 25 mL flask equipped with a reflux condenser was successively charged with 1′-(diphenylphosphino)-1-aminoferrocene (**2**; 770 mg, 2.0 mmol), triethyl orthoformate (10 mL, 60 mmol), and glacial acetic acid (17 μL, 0.3 μmol). The flask was transferred to an oil bath maintained at 155 °C, and the mixture was heated at reflux for 3 h. After cooling to room temperature, the ethanol and excess triethyl orthoformate were removed under vacuum (3×10^{-3} Torr, 55 °C). The dark red-brown residue was dissolved in isopropylamine (10 mL, 116 mmol), and the resulting mixture was refluxed overnight and then concentrated under vacuum. The brown oily residue was dissolved in dichloromethane (20 mL), and the solution was evaporated with chromatographic silica (10 g). The crude, preadsorbed product was purified by flash chromatography over silica gel on a Büchi Reveleris X2 chromatograph (80-g column, flow rate 30 mL min^{-1}, gradient from pure CH_2Cl_2 to CH_2Cl_2–MeOH 1 : 1, UV detection at 254, 265, and 280 nm). The second orange band was collected and evaporated. The residue was crystallised from hot heptane to produce amidine **1** as orange crystals. Note: the best yields were obtained when the hot solution was treated with a small amount of charcoal and filtered before crystallisation by slow cooling. Yield: 400 mg (43%). The crystal used for structure determination was selected from the preparative batch.

^{1}H NMR (DMSO-d_6, 400 MHz): δ 1.09 (d, $^3J_{HH}$ = 6.5 Hz, 6 H, CH*Me*$_2$), 3.74 (vt, J' = 1.9 Hz, 2 H, C_5H_4), 3.78–3.90 (br s, 1 H, CH*Me*$_2$), 3.93 (vq, J' = 1.9 Hz, 2 H, C_5H_4), 4.01 (vt, J' = 1.9 Hz, 2 H, C_5H_4), 4.30 (vt, J' = 1.8 Hz, 2 H, C_5H_4), 6.71 (br s, 1 H, NH), 7.27–7.39 (m, 10 H, PPh_2), 7.70 (s, 1 H, amidine CH). ^{13}C{^{1}H} NMR (DMSO-d_6, 101 MHz): δ 22.32 (s, 2 C, CH*Me*$_2$), 41.25 (s, 1 C, *C*HMe$_2$), 61.60 (s, 2 C, CH of C_5H_4), 65.21 (s, 2 C, CH of C_5H_4), 71.86 (d, J_{PC} = 4 Hz, 2 C, CH of C_5H_4), 72.80 (d, J_{PC} = 15 Hz, 2 C, CH of C_5H_4), 74.81 (d, J_{PC} = 7 Hz, 1 C, C^{ipso}–P of C_5H_4), 111.12 (s, 1 C, C^{ipso}–N of C_5H_4), 128.18 (d, J_{PC} = 7 Hz, 4 C, CH^{ortho} PPh_2), 128.40 (s, 2 C, CH^{para} PPh_2), 132.99 (d, J_{PC} = 19 Hz, 4 C, CH^{meta} PPh_2), 139.08 (d, J_{PC} = 11 Hz, 2 C, C^{ipso}–P PPh_2), 150.51 (s, 1 C, amidine CH). ^{31}P{^{1}H} NMR (DMSO-d_6, 162 MHz): δ −18.3 (s). ESI+ MS: *m*/*z* 454.1 (M^+). Anal. calc. for $C_{26}H_{27}FeN_2P$ (454.32): C 68.73, H 5.99, N 6.17%. Found: C 68.62, H 5.71, N 6.21%.

Preparation of [$NiCl_2$(1-κ^{2}P,N)] (3). [$NiCl_2$(dme)] (21.9 mg, 0.10 mmol) was dissolved in absolute ethanol (3 mL) in an oven-dried and nitrogen-filled Schlenk tube equipped with a stirring bar. The solution was frozen in liquid nitrogen and layered with a solution of ligand **1** (45.4 mg, 0.10 mmol) in dry acetone (3 mL). The mixture was kept at 4 °C for 48 hours, whereupon it thawed and deposited dark crystals, which were collected by suction and dried under vacuum. Yield of **3** : 31 mg (53%), black crystals. The crystal used for structure determination was obtained *via* reactive diffusion. Specifically, the solution of the metal precursor in absolute ethanol was frozen in liquid nitrogen and layered with a solution of **1** in acetone (Ni : **1** = 1 : 1) in a dry Schlenk tube. The mixture was set aside for crystallisation by liquid-phase diffusion in a refrigerator (4 °C).

ESI+ MS: *m*/*z* 547 ($[M - Cl]^+$), 455 ($[\mathbf{1} + H]^+$). HRMS (ESI+) *m*/*z* calc. for $C_{26}H_{27}ClFeN_2NiP$ ($[M - Cl]^+$): 547.0298, found: 547.0301. Anal. calc. for $C_{26}H_{27}Cl_2FeN_2NiP$ (583.93): C 53.48, H 4.66, N 4.80%. Found: C 53.48, H 4.60, N 4.43%.

Preparation of [$PdCl_2$(1-κ^{2}P,N)] (4). Ligand **1** (182 mg, 0.40 mmol) and [$PdCl_2$(MeCN)$_2$] (104 mg, 0.40 mmol) were dissolved in dry dichloromethane (5 mL). The resulting solution was stirred overnight and then filtered through a PTFE syringe filter (0.45 μm pore size) into 25 mL of cold pentane. The formed precipitate was allowed to settle, and the supernatant was decanted. The solid was dried under vacuum, leaving solvated **4** as a brick-red powder. Yield of **4**·$\frac{1}{2}CH_2Cl_2$: 251 mg (93%). Single crystals were grown by layering a dichloromethane solution of the complex with hexane.

^{1}H NMR (1,2-$C_2D_4Cl_2$, 300 MHz, 25 °C): δ 1.35 (br d, $^3J_{HH} \approx$ 6.5 Hz, 6 H, CH*Me*$_2$), 3.62 (br sept, $^3J_{HH} \approx$ 6.5 Hz, 1 H, CH*Me*$_2$), 3.97 (br s, 1 H, C_5H_4), 4.29 (br s, 1 H, C_5H_4), 4.38–4.59 (m, 3 H, C_5H_4), 4.67 (br s, 1 H, C_5H_4), 5.31 (br s, 2 H, C_5H_4), 7.09–7.70 (m, 10 H, PPh_2), 8.02 (br s, 2 H, amidine CH + NH). ^{1}H NMR (1,2-$C_2D_4Cl_2$, 300 MHz, −25 °C): δ 1.31 (d, $^3J_{HH}$ = 6.5 Hz, 3 H, CH*Me*$_2$), 1.34 (d, $^3J_{HH}$ = 6.7 Hz, 3 H, CH*Me*$_2$), 3.61 (sept, $^3J_{HH}$ = 6.7 Hz, 1 H, CH*Me*$_2$), 3.94 (br s, 1 H, C_5H_4), 4.28 (br s, 1 H, C_5H_4), 4.45 (br s, 2 H, C_5H_4), 4.53 (br s, 1 H, C_5H_4), 4.70 (br s, 1 H, C_5H_4), 5.28 (br s, 1 H, C_5H_4), 5.31 (br s, 1 H, C_5H_4), 7.08 (dd, J = 13.0, 8.3 Hz, 1 H, PPh_2), 7.18–7.42 (m, 6 H, PPh_2), 7.51 (m, 2 H, PPh_2), 7.62 (m, 1 H, PPh_2), 7.97 (dd, J = 12.1, 7.6 Hz, 2 H, amidine CH + NH). ^{13}C{^{1}H} NMR (1,2-$C_2D_4Cl_2$, 75 MHz, 25 °C): δ 23.58 (s, 2 C, CH*Me*$_2$), 48.90 (s, 1 C, *C*HMe$_2$), 65.83 (br s, 1 C, CH of C_5H_4), 66.36 (br s, 2 C, CH of C_5H_4), 69.27 (br s, 1 C, CH of C_5H_4), 71.20–71.99 (m, 2 C, C^{ipso}–P and CH of C_5H_4), 73.98 (br s, 1 C, CH of C_5H_4), 75.55 (br s, 1 C, CH of C_5H_4), 76.47 (br s, 1 C, CH of C_5H_4), 113.41 (s, 1 C, C^{ipso}–N of C_5H_4), 127.25–128.93 (m, 5 C, C^{ipso}–P PPh_2 + 4 CH PPh_2), 130.11 (br s, 1 C, CH^{para} PPh_2), 131.51–133.04 (m, 4 C, C^{ipso}–P PPh_2 + 2 CH PPh_2 + CH^{para} PPh_2), 134.88 (br s, 2 C, CH PPh_2), 157.88 (s, 1 C, amidine CH). ^{13}C{^{1}H} NMR (1,2-$C_2D_4Cl_2$, 75 MHz, −25 °C): δ 23.43 (s, 1 C, CH*Me*$_2$), 24.06 (s, 1 C, CH*Me*$_2$), 49.17 (s, 1 C, *C*HMe$_2$), 65.88 (s, 1 C, CH of C_5H_4), 66.41 (d, J_{PC} = 21 Hz, 2 C, C_5H_4), 69.34 (s, 1 C, CH of C_5H_4), 71.29 (d, J_{PC} = 64 Hz, 1 C, C^{ipso}–P of C_5H_4), 71.66 (s, 1 C, CH of C_5H_4), 74.25 (d, J_{PC} = 9 Hz, 1 C, CH of C_5H_4), 75.71 (d, J_{PC} = 5 Hz, 1 C, CH of C_5H_4), 76.45 (d, J_{PC} = 18 Hz, 1 C, CH of C_5H_4), 113.64 (d, J_{PC} = 2 Hz, 1 C, C^{ipso}–N of C_5H_4), 127.71

(d, J_{PC} = 11 Hz, 2 C, CH PPh_2), 128.57 (d, J_{PC} = 54 Hz, 1 C, C^{ipso}–P PPh_2), 128.58 (d, J_{PC} = 11 Hz, 2 C, CH PPh_2), 130.19 (s, 1 C, CH^{para} PPh_2), 132.00 (s, 1 C, CH^{para} PPh_2), 132.26 (d, J_{PC} = 10 Hz, 2 C, CH PPh_2), 132.75 (d, J_{PC} = 58 Hz, 1 C, C^{ipso}–P PPh_2), 134.83 (d, J_{PC} = 12 Hz, 2 C, CH PPh_2), 158.09 (s, 1 C, amidine CH). $^{31}P\{^1H\}$ NMR (1,2-$C_2D_4Cl_2$, 121 MHz, 25 °C): δ 28.8 (s). MALDI-TOF MS: m/z 596.93 ($[M - Cl]^+$). Anal. calc. for $C_{26}H_{27}Cl_2FeN_2PPd\cdot\frac{1}{2}CH_2Cl_2$ (674.1): C 47.21, H 4.19, N 4.16%. Found: C 46.96, H 4.09, N 3.99%.

Preparation of [$PtCl_2$(1-κ^{2}P,N)] (5). Ligand **1** (45.4 mg, 0.10 mmol) and [$PtCl_2$(cod)] (37.4 mg, 0.10 mmol) were mixed in dichloromethane (2 mL). The resulting solution was stirred for 30 min and filtered through a PTFE filter (0.45 μm porosity) into a 25 mL test tube. The filtrate was layered with 1 mL of CH_2Cl_2 and then with an excess of hexane. Crystallisation by liquid-phase diffusion over several days produced complex **5** as yellow crystals, which were filtered off, washed with pentane, and dried under vacuum. Yield of **5**·$\frac{1}{2}CH_2Cl_2$: 46.4 mg (61%). The crystal used for single-crystal X-ray diffraction analysis was grown from dichloromethane/hexane.

^{1}H NMR (CD_2Cl_2, 400 MHz): δ 1.38 (d, $^3J_{HH}$ = 6.6 Hz, 3 H, CHMe_2), 1.41 (d, $^3J_{HH}$ = 6.6 Hz, 3 H, CHMe_2), 3.67 (sept, $^3J_{HH}$ = 6.6 Hz, 1 H, CHMe_2), 3.94 (vd, J' = 1.4 Hz, 1 H, C_5H_4), 4.25 (m, 1 H, C_5H_4), 4.28 (m, 1 H, C_5H_4), 4.38 (m, 1 H, C_5H_4), 4.41 (s, 1 H, C_5H_4), 4.67 (vt, J' = 1.6 Hz, 1 H, C_5H_4), 5.17 (m, 1 H, C_5H_4), 5.26 (m, 1 H, C_5H_4), 7.25–7.38 (m, 7 H, NH + amidine CH + 5 H of PPh_2), 7.42–7.49 (m, 2 H, PPh_2), 7.53–7.60 (m, 1 H, PPh_2), 7.90–7.98 (m, 2 H, PPh_2). $^{13}C\{^1H\}$ NMR (CD_2Cl_2, 101 MHz): δ 23.73 (s, 1 C, CHMe_2), 24.27 (s, 1 C, CHMe_2), 49.38 (s, 1 C, CHMe$_2$), 65.87 (s, 1 C, CH of C_5H_4), 66.40 (s, 1 C, CH of C_5H_4), 66.44 (s, 1 C, CH of C_5H_4), 69.13 (s, 1 C, CH of C_5H_4), 71.83 (s, J_{PC} = 70 Hz, 1 C, C^{ipso}–P of C_5H_4), 71.91 (d, J_{PC} = 7 Hz, 1 C, CH of C_5H_4), 74.14 (d, J_{PC} = 9 Hz, 1 C, CH of C_5H_4), 75.08 (d, J_{PC} = 6 Hz, 1 C, CH of C_5H_4), 76.55 (d, J_{PC} = 16 Hz, 1 C, CH of C_5H_4), 113.35 (s, 1 C, C^{ipso}–N of C_5H_4), 127.81 (d, J_{PC} = 12 Hz, 2 C, CH^{meta} PPh_2), 128.62 (d, J_{PC} = 11 Hz, 2 C, CH^{meta} PPh_2), 130.42 (d, J_{PC} = 2 Hz, 1 C, CH^{para} PPh_2), 131.33 (d, J_{PC} = 65 Hz, 1 C, C^{ipso}–P PPh_2), 132.09 (d, J_{PC} = 2 Hz, 1 C, CH^{para} PPh_2), 132.89 (d, J_{PC} = 10 Hz, 2 C, CH^{ortho} PPh_2), 135.28 (d, J_{PC} = 12 Hz, 2 C, CH^{ortho} PPh_2), 156.98 (s, 1 C, amidine CH). $^{31}P\{^1H\}$ NMR (CD_2Cl_2, 162 MHz): δ 5.3 (s with ^{195}Pt satellites, $^1J_{PtP}$ = 2042 Hz). MALDI-TOF MS: m/z 685.0 ($[M - Cl]^+$). Anal. calc. for $C_{26}H_{27}Cl_2FeN_2PPt\cdot\frac{1}{2}CH_2Cl_2$ (762.78): C 41.73, H 3.70, N 3.67%. Found: C 41.71, H 3.39, N 3.56%.

Synthesis of [PdCl(Me)(1-κ^{2}P,N)] (6). Ligand **1** (45.4 mg, 0.10 mmol) and [PdClMe(cod)] (24.6 mg, 0.10 mmol) were dissolved in anhydrous dichloromethane (2 mL). The solution was stirred for 30 min and filtered through a PTFE syringe filter (0.45 μm pore size). The filtrate was layered with hexane and set aside for crystallisation by liquid-phase diffusion. The crystals that formed over several days were filtered off and dried under vacuum. Yield of **6**: 37 mg (61%), light yellow crystals. A crystal suitable for structure determination was obtained from dichloromethane/hexane.

^{1}H NMR (CD_2Cl_2, 400 MHz): δ 0.33 (d, J_{PH} = 4.2 Hz, 3 H, PdMe), 1.37 (d, J_{HH} = 6.5 Hz, 6 H, CHMe_2), 3.57 (sept, J_{HH} = 6.9 Hz, 6 H, CHMe_2), 3.98 (vt, J' = 2.0 Hz, 2 H, C_5H_4), 4.36 (vt, J' = 1.9 Hz, 2 H, C_5H_4), 4.45 (vtd, J' = 1.9, 0.7 Hz, 2 H, C_5H_4), 4.60 (vq, J' = 2.1 Hz, 2 H, C_5H_4), 7.21 (dd, $^3J_{HH}$ = 12.1, 7.6 Hz, 1 H, NH), 7.33–7.40 (m, 5 H, 4 CH PPh_2 + amidine), 7.40–7.46 (m, 2 H, PPh_2), 7.52–7.59 (m, 4 H, PPh_2). $^{13}C\{^1H\}$ NMR (CD_2Cl_2, 101 MHz): δ 3.08 (d, J_{PC} = 4 Hz, 1 C, PdMe), 24.33 (s, 2 C, CHMe_2), 48.25 (s, 1 C, CHMe$_2$), 64.89 (s, 2 C, CH of C_5H_4), 66.92 (s, 2 C, CH of C_5H_4), 72.01 (d, J_{PC} = 7 Hz, 2 C, CH of C_5H_4), 74.59 (d, J_{PC} = 54 Hz, 1 C, C^{ipso}–P C_5H_4), 75.00 (d, J_{PC} = 12 Hz, 2 C, CH of C_5H_4), 113.84 (d, J_{PC} = 2 Hz, 1 C, C^{ipso}–N of C_5H_4), 128.30 (d, J_{PC} = 11 Hz, 4 C, CH^{ortho} PPh_2), 130.66 (d, J_{PC} = 3 Hz, 2 C, CH^{para} PPh_2), 133.02 (d, J_{PC} = 51 Hz, 2 C, C^{ipso}–P PPh_2), 134.42 (d, $^3J_{PC}$ = 12 Hz, 4 C, CH^{meta} PPh_2), 157.47 (s, 1 C, amidine CH). $^{31}P\{^1H\}$ NMR (CD_2Cl_2, 162 MHz): δ 32.6 (s). ESI+ MS: m/z 575 ($[M - Cl]^+$). Anal. calc. for $C_{27}H_{30}ClFeN_2PPd\cdot0.2CH_2Cl_2$ (628.2): C 52.00, H 4.88, N 4.46%. Found: C 52.29, H 4.59, N 4.19%.

[Pd(μ-Cl)(1-κ^{2}P,N)]$_2$[BARF]$_2$ (7). Solid sodium tetrakis(3,5-bis(trifluoromethyl)phenyl)borate (177.2 mg, 0.20 mmol) was added to a solution of complex **4** (126.8 mg, 0.20 mmol) in anhydrous dichloromethane (5 mL). The colour of the reaction mixture immediately changed from red to green. The mixture was stirred for 1 h and filtered through a PTFE syringe filter (0.45 μm porosity). The filtrate was evaporated under vacuum, and the green residue was dissolved in dichloromethane (5 mL) under gentle warming. The dark red-brown solution was transferred to a 25 mL test tube and layered with hexane. Crystallisation by liquid-phase diffusion over several days produced green crystals, which were filtered off, washed with cold pentane, and dried under vacuum. Yield of **7**: 132 mg (45%), green crystals.

$^{31}P\{^1H\}$ NMR (acetone-d_6, 162 MHz): δ −7.6 (s), 36.3 (br s), ≈38.3 and 39.3 (2× br s). $^{31}P\{^1H\}$ NMR (CD_2Cl_2, 162 MHz): δ −9.5 (s). ESI+ MS: m/z 595 ($[Pd(\mathbf{1})Cl]^+$), 559 ($[Pd(\mathbf{1})Cl - HCl]^+$). Anal. calc. for $C_{116}H_{78}B_2Cl_2F_{48}Fe_2N_4P_2Pd_2$ (2918.82): C 47.73, H 2.69, N 1.92%. Found: C 47.82, H 2.25, N 1.89%.

[(μ-Cl){PdCl(1-κ^{2}P,N)}$_2$][BF_4] (9). Complex **4** (63.2 mg, 0.10 mmol) was dissolved in anhydrous dichloromethane (5 mL), and solid Ag[BF_4] (9.8 mg, 0.050 mmol) was added. The turbid mixture was stirred in the dark for 2 h and then filtered through a PTFE syringe filter (0.45 μm porosity). The red filtrate was layered with hexane and set aside for crystallisation by slow liquid-phase diffusion. After several days, the separated solid was filtered off, washed with cold pentane, and dried under vacuum to yield **9** as dark red crystals. Yield: 58 mg (84%). The crystal used for structure determination was selected from the preparative batch (before isolation).

^{1}H NMR (1,2-$C_2D_4Cl_2$, 300 MHz, 25 °C): δ 1.32 (d, $^3J_{HH}$ = 6.6 Hz, 3 H, CHMe_2), 1.52 (s, 3 H, CHMe_2), 3.61 (m, 1 H, CHMe_2), 4.01 (s, 1 H, C_5H_4), 4.33 (s, 1 H, C_5H_4), 4.58 (s, 1 H, C_5H_4), 4.63 (s, 1 H, C_5H_4), 4.75 (s, 2 H, C_5H_4), 5.26 (br s, 2 H, C_5H_4), 7.18 (br d, J = 13.3 Hz, 1 H, PPh_2), 7.32–7.70 (m, 7 H, PPh_2), 8.13 (dd, J = 12.7, 7.8 Hz, 2 H, PPh_2), 8.79 (br s, 1 H, amidine CH). ^{1}H NMR (1,2-$C_2D_4Cl_2$, 300 MHz, −25 °C): δ 1.28 (d, $^3J_{HH}$ = 6.5 Hz, 3 H, CHMe_2), 1.52 (d, $^3J_{HH}$ = 6.3 Hz, 3 H, CHMe_2), 3.58 (m, 1 H, CHMe_2), 3.95 (s, 1 H, isomer B, CH of C_5H_4), 4.00 (s, 1 H, isomer A, CH of C_5H_4), 4.27 (s, 1 H, isomer B, CH of C_5H_4), 4.33 (s, 1 H, isomer A, CH of

C_5H_4), 4.49 (s, 1 H, isomer B, CH of C_5H_4), 4.58 (s, 1 H, isomer A, CH of C_5H_4), 4.65 (s, 1 H, isomer A, CH of C_5H_4), 4.72 (s, 1 H, isomer A, CH of C_5H_4), 4.76 (s, 1 H, isomer A, CH of C_5H_4), 5.16 (s, 1 H, isomer A, CH of C_5H_4), 5.23 (s, 1 H, isomer A, CH of C_5H_4), 5.34 (s, 2 H, isomer B, CH of C_5H_4), 7.19 (d, J = 13.2 Hz, 1 H, PPh_2), 7.32–7.67 (m, 7 H, PPh_2), 8.10 (dd, J = 12.6, 7.7 Hz, PPh_2), 8.78 (dd, J = 13.3, 8.7 Hz, 1 H, NH), 9.26 (br s, 1 H, amidine CH). ^{19}F NMR (acetone-d_6, 376 MHz, 25 °C): −152.7 (br s). $^{31}P\{^1H\}$ NMR (1,2-$C_2D_4Cl_2$, 121 MHz, 25 °C): δ 31.2 (br s, isomer B), 32.9 (s, isomer A). ESI+ MS: 597 ($[LPdCl]^+$), 1227 ($[M - BF_4]^+$). Anal. calc. for $C_{52}H_{54}BCl_3F_4Fe_2N_4P_2Pd_2{\cdot}0.8CH_2Cl_2$ (1382.60): C 45.87, H 4.05, N 4.05%. Found: C 45.89, H 3.98, N 3.94%.

[Pd(1-κ^{3}Fe,P,N)(PPh$_3$)][BF$_4$]$_2$ (10-BF$_4$). Ligand **1** (45.4 mg, 0.10 mmol) and triphenylphosphine (26.0 mg, 0.10 mmol) were dissolved in acetone (3 mL). In a separate flask, $[Pd(MeCN)_4][BF_4]_2$ (44.4 mg, 0.10 mmol) was dissolved in the same solvent (4 mL), and the two solutions were combined and stirred for 30 min. The dark red mixture was evaporated under vacuum. The residue was dissolved in dichloromethane (2 mL) and layered with diethyl ether to induce crystallisation. The crystals, which formed over several days, were filtered off, washed with cold pentane, and dried under vacuum. Yield of **10**-BF_4: 73 mg (73%), dark red crystals. The crystal used for structure determination was obtained from dichloromethane/diethyl ether.

^{1}H NMR (CD_2Cl_2, 400 MHz): δ 0.95 (br d, $^3J_{HH}$ = 6.5 Hz, 6 H, CHMe_2), 3.13 (sept, $^3J_{HH}$ = 6.5 Hz, 1 H, CHMe_2), 3.48 (vq, J' = 2.4 Hz, 2 H, C_5H_4), 4.04 (s, 2 H, C_5H_4), 5.68 (vt, J' = 2.2 Hz, 2 H, C_5H_4), 5.80 (vq, J' = 1.9 Hz, 2 H, C_5H_4), 6.31 (br s, 1 H), 6.88 (br s, 1 H), 7.33–7.40 (m, 4 H, CH PPh_2 and PPh_3), 7.42–7.59 (m, 21 H, CH PPh_2 and PPh_3). $^{13}C\{^1H\}$ NMR (CD_2Cl_2, 101 MHz): δ 22.69 (s, 2 C, CHMe_2), 50.61 (s, 1 C, CHMe$_2$), 68.14 (s, 2 C, CH of C_5H_4), 72.51 (d, J_{PC} = 11 Hz, 2 C, CH of C_5H_4), 82.32 (s, 2 C, CH of C_5H_4), 86.71 (d, J_{PC} = 8 Hz, 2 C, CH of C_5H_4), 119.70 (dd, J_{PC} = 65 and 4 Hz, 2 C, C^{ipso}–P of PPh_2), 128.89 (d, J_{PC} = 49 Hz, 3 C, C^{ipso}–P PPh_3), 130.19 (d, J_{PC} = 13 Hz, 4 C, CH^{ortho} PPh_2), 130.35 (d, J_{PC} = 12 Hz, 6 C, CH^{meta} PPh_3), 133.29 (d, J_{PC} = 3 Hz, 3 C, CH^{para} PPh_3), 133.92 (d, J_{PC} = 3 Hz, 2 C, CH^{para} PPh_2), 134.73 (d, J_{PC} = 12 Hz, 6 C, CH^{ortho} PPh_3), 135.39 (d, J_{PC} = 13 Hz, 4 C, CH^{meta} PPh_2), 154.21 (s, 1 C, amidine CH); the signals due to ferrocene C^{ipso} were not detected. ^{19}F NMR (CD_2Cl_2, 376 MHz): δ −150.73 (s, $[^{10}BF_4]^-$, 20%), −150.79 (s, $[^{11}BF_4]^-$, 80%). $^{31}P\{^1H\}$ NMR (CD_2Cl_2, 162 MHz): δ −6.6 (br s, PPh_2), 31.0 (d, $^2J_{PP}$ = 25 Hz, PPh_3). ESI+ MS: m/z 411 ($[M - 2BF_4]^{2+}$), 821 ($[M - 2BF_4 - H]^+$). Anal. calc. for $C_{44}H_{42}B_2F_8FeN_2P_2Pd$ (996.65): C 53.03, H 4.25, N 2.81%. Found: C 52.99, H 4.00, N 2.81%.

[Pd(1-κ^{3}Fe,P,N)(PPh$_3$)][PF$_6$]$_2$ (10-PF$_6$). Complex **10**-BF_4 (71.5 mg, 0.072 mmol) was dissolved in dichloromethane (5 mL). The solution was transferred to a small separatory funnel and washed twice with aqueous $Na[PF_6]$ (336 mg, 2.0 mmol were dissolved in 5 mL distilled water, and the solution was divided into two 2.5-mL portions). The organic layer was separated, dried over anhydrous magnesium sulfate, filtered, and concentrated under vacuum. The residue was dissolved in dichloromethane (3 mL), and the solution was layered with diethyl ether in a test tube. The crystals, which formed after several days, were filtered off and dried under vacuum. Yield of **10**-$PF_6{\cdot}0.4CH_2Cl_2$: 40 mg (48%), dark red crystals. The crystal used for structure determination was grown from dichloromethane/diethyl ether.

^{1}H NMR (acetone-d_6, 400 MHz): δ 0.98 (d, $^3J_{HH}$ = 6.6 Hz, 6 H, CHMe_2), 3.27 (sept, $^3J_{HH}$ = 6.6 Hz, 1 H, CHMe_2), 3.53 (vq, J' = 1.9 Hz, 2 H, C_5H_4), 4.09 (vt, J' = 2.2 Hz, 2 H, C_5H_4), 5.87 (vt, J' = 2.2 Hz, 2 H, C_5H_4), 6.04 (vq, J' = 1.8 Hz, 2 H, C_5H_4), 6.64 (br s, 1 H, amidine), 7.42–7.67 (m, 4 H, PPh_2 and PPh_3), 7.52–7.58 (m, 6 H, PPh_2 and PPh_3), 7.62–7.73 (m, 16 H, PPh_2 and PPh_3), 8.45 (br s, 1 H, NH). $^{13}C\{^1H\}$ NMR (acetone-d_6, 101 MHz): δ 22.89 (s, 2 C, CHMe_2), 51.10 (s, 1 C, CHMe$_2$), 54.35 (s, J_{PC} = 49 Hz, 1 C, C^{ipso}–P of C_5H_4), 68.68 (s, 2 C, CH of C_5H_4), 72.87 (d, J_{PC} = 11 Hz, 2 C, CH of C_5H_4), 82.71 (s, 2 C, CH of C_5H_4), 87.62 (d, J_{PC} = 8 Hz, 2 C, CH of C_5H_4), 120.48 (dd, J_{PC} = 64 and 4 Hz, 2 C, C^{ipso}–P PPh_2), 129.77 (d, J_{PC} = 49 Hz, 3 C, C^{ipso}–P PPh_3), 130.62 (d, J_{PC} = 13 Hz, 4 C, CH^{ortho} PPh_2), 130.77 (d, J_{PC} = 12 Hz, 6 C, CH^{meta} PPh_3), 133.78 (d, J_{PC} =3 Hz, 2 C, CH^{para} PPh_2), 134.42 (d, J_{PC} = 3 Hz, 3 C, CH^{para} PPh_3), 135.41 (d, J_{PC} = 12 Hz, 6 C, CH^{ortho} PPh_3), 136.13 (d, J_{PC} = 13 Hz, 4 C, CH^{meta} PPh_2), 155.27 (s, 1 C, amidine CH); the signal due to C^{ipso}–N of C_5H_4 was not observed. ^{19}F NMR (acetone-d_6, 376 MHz): δ −72.3 (d, $^1J_{FP}$ = 708 Hz, $[PF_6]^-$). $^{31}P\{^1H\}$ NMR (acetone-d_6, 162 MHz): δ −144.3 (sept, J_{FP} = 708 Hz, $[PF_6]^-$), −6.3 (d, J_{PP} = 26 Hz, PPh_2), 31.5 (d, J_{PP} = 26 Hz, PPh_3). ESI+ MS: m/z 411 ($[M - 2PF_6]^{2+}$), 821 ($[M - 2PF_6 - H]^+$). Anal. calc. for $C_{44}H_{42}B_2F_8FeN_2P_2Pd{\cdot}0.4CH_2Cl_2$ (1146.93): C 46.50, H 3.76, N2.44%. Found: C 46.83, H 3.44, N 2.40%.

[Pd(1-κ^{2}P,N)(η^2-ma)] (11). Ligand **1** (45.4 mg, 0.10 mmol) and [Pd(ma)(N^N)] (37.3 mg, 0.10 mmol) were dissolved in anhydrous dichloromethane (2 mL). The solution was transferred into a 25 mL test tube and layered with 1 mL of dry CH_2Cl_2 and subsequently with 5 mL of dry hexane. Crystallisation by liquid-phase diffusion over several days produced orange crystals, which were filtered off, washed with cold pentane, and dried under vacuum. Yield of **11**: 50 mg (76%), orange crystals.

ESI+ MS: m/z 597 ($[M - C_4H_2O_3 + Cl]^+$), 559 ($[M - C_4H_2O_3]]^+$ (recorded in CH_2Cl_2). ESI+ HRMS: m/z calc. for $C_{30}H_{30}FeN_2O_3PPd$ ($[M + H]^+$): 659.0378, found: 659.0301. Anal. calc. for $C_{30}H_{29}FeN_2O_3PPd{\cdot}0.2CH_2Cl_2$ (675.8): C 53.67, H 4.39, N 4.15%. Found: C 53.98, H 4.23, N 4.07%. The NMR spectra could not be recorded because the compound is only very poorly soluble in common deuterated solvents. Nevertheless, the $^{31}P\{^1H\}$ NMR spectrum of the reaction mixture in CD_2Cl_2 exhibited a singlet at δ_P 20 ppm as the sole signal (see the SI). The crystal suitable for structure determination was selected from the preparative batch.

Conflicts of interest

There are no conflicts of interest to declare.

Data availability

The data supporting this article have been included as part of the SI. Supplementary information: Additional structure

diagrams and crystallographic details, magnetochemical data, and copies of the NMR spectra. See DOI: https://doi.org/10.1039/d5nj02886h

CCDC 2469284–2469293 contain the supplementary crystallographic data for this paper.[42–51]

Acknowledgements

The authors acknowledge support from the Czech Science Foundation (project no. 23-06718S).

References

1 (*a*) C. S. Slone, D. A. Weinberger and C. A. Mirkin, *Progr. Inorg. Chem.*, 1999, **48**, 233; (*b*) P. Braunstein and F. Naud, *Angew. Chem., Int. Ed.*, 2001, **40**, 680.

2 (*a*) M. P. Carroll and P. J. Guiry, *Chem. Soc. Rev.*, 2014, **43**, 819; (*b*) J. Margalef, M. Biosca, P. de la Cruz Sánchez, J. Faiges, O. Pàmies and M. Diéguez, *Coord. Chem. Rev.*, 2021, **446**, 214120.

3 (*a*) D. Astruc, *Eur. J. Inorg. Chem.*, 2017, 6; (*b*) P. Štěpnička, *Dalton Trans.*, 2022, **51**, 8085.

4 (*a*) R. C. J. Atkinson, V. C. Gibson and N. J. Long, *Chem. Soc. Rev.*, 2004, **33**, 313; (*b*) T. Nöel and J. Van der Eycken, *Green Process Synth.*, 2013, **2**, 297; (*c*) Š. Toma, J. Csizmadiová, M. Mečiarová and R. Šebesta, *Dalton Trans.*, 2014, **43**, 16557; (*d*) N. Dwadnia, J. Roger, N. Pirio, H. Cattey and J.-C. Hierso, *Coord. Chem. Rev.*, 2018, **355**, 74; (*e*) L. Cunningham, A. Benson and P. J. Guiry, *Org. Biomol. Chem.*, 2020, **18**, 9329.

5 (*a*) K.-S. Gan and T. S. A. Hor, in *Ferrocenes: Homogeneous Catalysis, Organic Synthesis Mater. Sci.*, ed. A. Togni and T. Hayashi, Wiley-VCH, Weinheim, Germany, 1995, ch. 1, pp. 3–104; (*b*) S. W. Chien and T. S. A. Hor, in *Ferrocenes: Ligands, Materials and Biomolecules*, ed. P. Štěpnička, Wiley, Chichester, UK, 2008, ch. 2, pp. 33–116; (*c*) T. J. Colacot and S. Parisel, in *Ferrocenes: Ligands, Materials and Biomolecules*, ed. P. Štěpnička, Wiley, Chichester, UK, 2008, ch. 3, pp. 117–140; (*d*) G. Bandoli and A. Dolmella, *Coord. Chem. Rev.*, 2000, **209**, 161; (*e*) D. J. Young, S. W. Chien and T. S. A. Hor, *Dalton Trans.*, 2012, **41**, 12655; (*f*) S. Dey and R. Pietschnig, *Coord. Chem. Rev.*, 2021, **437**, 213850.

6 (*a*) I. R. Butler and S. C. Quayle, *J. Organomet. Chem.*, 1998, **552**, 63; (*b*) M. Ritte, C. Bruhn and U. Siemeling, *Z. Naturforsch.*, 2014, **69b**, 906; (*c*) K. Škoch, I. Císařová, J. Schulz, U. Siemeling and P. Štěpnička, *Dalton Trans.*, 2017, **46**, 10339; (*d*) S. Dey, F. Roesler, C. Bruhn, Z. Kelemen and R. Pietschnig, *Inorg. Chem. Front.*, 2023, **10**, 3828.

7 For derived compounds, see: (*a*) $Ph_2PfcNHSO_2Me$ – V. Varmužová, F. Horký and P. Štěpnička, *New J. Chem.*, 2021, **45**, 3319; (*b*) $Ph_2PfcNHCX_2CH_2PPh_2$ (X = O and H_2) – M. Navrátil, I. Císařová and P. Štěpnička, *Dalton Trans.*, 2022, **51**, 14618.

8 (*a*) T. Yoshida, K. Tani, T. Yamagata, Y. Tatsuno and T. Saito, *J. Chem. Soc., Chem. Commun.*, 1990, **292**; (*b*) I. R. Butler, *Organometallics*, 1992, **11**, 74; (*c*) P. Štěpnička, J. Schulz, T. Klemann, U. Siemeling and I. Císařová, *Organometallics*, 2010, **29**, 3187; (*d*) U. Siemeling, T. Klemann, C. Bruhn, J. Schulz and P. Štěpnička, *Dalton Trans.*, 2011, **40**, 4722.

9 (*a*) K. Škoch, I. Císařová and P. Štěpnička, *Inorg. Chem.*, 2014, **53**, 568; (*b*) K. Škoch, I. Císařová and P. Štěpnička, *Chem. – Eur. J.*, 2015, **21**, 15998; (*c*) K. Škoch, F. Uhlík, I. Císařová and P. Štěpnička, *Dalton Trans.*, 2016, **45**, 10655; (*d*) K. Škoch, F. Uhlík, I. Císařová and P. Štěpnička, *Dalton Trans.*, 2018, **47**, 16082; (*e*) O. Bárta, I. Císařová, J. Schulz and P. Štěpnička, *New J. Chem.*, 2019, **43**, 11258.

10 (*a*) Z. Weng, S. Teo, L. L. Koh and T. S. A. Hor, *Organometallics*, 2004, **23**, 4342; (*b*) Z. Weng, S. Teo, L. L. Koh and T. S. A. Hor, *Angew. Chem., Int. Ed.*, 2005, **44**, 7560; (*c*) Z. Weng, S. Teo, L. L. Koh and T. S. A. Hor, *Chem. Commun.*, 2006, 1319; (*d*) Z. Weng, S. Teo and T. S. A. Hor, *Organometallics*, 2006, **25**, 4878; (*e*) Z. Weng, S. Teo, Z.-P. Liu and T. S. A. Hor, *Organometallics*, 2007, **26**, 2950.

11 (*a*) O. B. Sutcliffe and M. R. Bryce, *Tetrahedron: Asymmetry*, 2003, **14**, 2297; (*b*) Y. Miyake, Y. Nishibayashi and S. Uemura, *Synlett*, 2008, 1747; (*c*) G. C. Hargaden and P. J. Guiry, *Chem. Rev.*, 2009, **109**, 2505; (*d*) R. Connon, B. Roche, B. V. Rokade and P. J. Guiry, *Chem. Rev.*, 2021, **121**, 6373 and references cited therein.

12 Selected examples: (*a*) W. Zhang, Y. Yoneda, T. Kida, Y. Nakatsuji and I. Ikeda, *Tetrahedron: Asymmetry*, 1998, **9**, 3371; (*b*) J. Park, Z. Quan, S. Lee, K. H. Ahn and C.-W. Cho, *J. Organomet. Chem.*, 1999, **584**, 140; (*c*) W.-P. Deng, S.-L. You, X.-L. Hou, L.-X. Dai, Y.-H. Yu, W. Xia and J. Sun, *J. Am. Chem. Soc.*, 2001, **123**, 6508; (*d*) T. Tu, W.-P. Deng, X.-L. Hou, L.-X. Dai and X.-C. Dong, *Chem. – Eur. J.*, 2003, **9**, 3073; (*e*) X.-X. Yan, Q. Peng, Y. Zhang, K. Zhang, W. Hong, X.-L. Hou and Y.-D. Wu, *Angew. Chem., Int. Ed.*, 2006, **45**, 1979.

13 (*a*) O. Bárta, R. Gyepes, I. Císařová, A. Alemayehu and P. Štěpnička, *Dalton Trans.*, 2020, **49**, 4225; (*b*) O. Bárta, I. Císařová and P. Štěpnička, *Dalton Trans.*, 2021, **50**, 14662.

14 (*a*) H. Charvátová, I. Císařová and P. Štěpnička, *Eur. J. Inorg. Chem.*, 2017, 288; (*b*) O. Bárta, I. Císařová and P. Štěpnička, *Eur. J. Inorg. Chem.*, 2017, 489; (*c*) O. Bárta, I. Císařová, E. Mieczyńska, A. M. Trzeciak and P. Štěpnička, *Eur. J. Inorg. Chem.*, 2019, 4846.

15 C. Binnani, Z. Leitner, I. Císařová and P. Štěpnička, *Eur. J. Inorg. Chem.*, 2024, e202300644.

16 For other phosphinoferrocene amidines, see: (*a*) X. P. Hu, H. Chen, X. Hu, H. Dai, C. Bai, J. Wang and Z. Zheng, *Tetrahedron Lett.*, 2002, **43**, 9179; (*b*) X. Hu, H. Chen, H. Dai, X. Hu and Z. Zheng, *Tetrahedron: Asymmetry*, 2003, **14**, 2073; (*c*) A. Bertogg and A. Togni, *Organometallics*, 2006, **25**, 622. For related compounds containing *ortho*-phenylene unit as the ligand backbone, see: (*d*) N. Tsukada, O. Tamura and Y. Inoue, *Organometallics*, 2002, **21**, 2521; (*e*) N. Tsukada, T. Mitsuboshi, H. Setoguchi and Y. Inoue, *J. Am. Chem. Soc.*, 2003, **125**, 12102; (*f*) N. Tsukada, S. Ninomiya, Y. Aoyama and Y. Inoue, *Org. Lett.*, 2007, **9**, 2919; (*g*) K. Son, D. M. Pearson, S.-J. Jeon and R. M. Waymouth, *Eur. J. Inorg. Chem.*,

2011, 4256; (*h*) N. Tsukada, N. Ohnishi, S. Aono and F. Takahashi, *Organometallics*, 2012, **31**, 7336; (*i*) X.-Q. Zhang and Z.-X. Wang, *J. Org. Chem.*, 2012, **77**, 3658; (*j*) Y. Yamaguchi, K. Yamanishi, M. Kondo and N. Tsukada, *Organometallics*, 2013, **32**, 4837; (*k*) R. Liu, K. Zhu, X. Zhong, J. Li, Z. Liu, S. Chen and H. Zhu, *Dalton Trans.*, 2016, **45**, 17020; (*l*) Z. Feng, Y. Jiang, H. Ruan, Y. Zhao, G. Tan, L. Zhang and X. Wang, *Dalton Trans.*, 2019, **48**, 14975; (*m*) M. Dahlen, T. P. Seifert, S. Lebedkin, M. T. Gamer, M. M. Kappes and P. W. Roesky, *Chem. Commun.*, 2021, **57**, 13146; (*n*) M. Dahlen, M. Kehry, S. Lebedkin, M. M. Kappes, W. Klopper and P. W. Roesky, *Dalton Trans.*, 2021, **50**, 13412; (*o*) M. Dahlen, N. Reinfandt, C. Jin, M. T. Gamer, K. Fink and P. W. Roesky, *Chem. – Eur. J.*, 2021, **27**, 15128; (*p*) Y. Yamamoto, T. Mommae, T. Fujimoto, M. Kondo and N. Tsukada, *Organometallics*, 2024, **43**, 4837.

17 M. R. Ringenberg, *Chem. – Eur. J.*, 2019, **25**, 2396.

18 For recent examples of analogous sequential syntheses but with isolated formamidine intermediates, see: (*a*) A. Binobaid, M. Iglesias, D. J. Beetstra, B. Kariuki, A. Dervisi, I. A. Fallis and K. J. Cavell, *Dalton Trans.*, 2009, 7099; (*b*) N. V. Kulkarni, T. Elkin, B. Tumanskii, M. Botoshansky, L. J. W. Shimon and M. S. Eisen, *Organometallics*, 2014, **33**, 3119.

19 (*a*) D. Guillaneux and H. B. Kagan, *J. Org. Chem.*, 1995, **60**, 2502; (*b*) A. Muller, S. Otto and A. Roodt, *Dalton Trans.*, 2008, 650.

20 S. I. Kirin, H.-B. Kraatz and N. Metzler-Nolte, *Chem. Soc. Rev.*, 2006, **35**, 348.

21 τ is the torsion angle C1–Cg1–Cg2–C6, where Cg1 and Cg2 denote the centroids of the cyclopentadienyl rings C(1–5) and C(6–10), respectively.

22 Most of the free amidines, whose crystal structure has been determined, bear a pair of aryl substituents at the N atoms. A compound relevant to the present structure is, for instance, DippCH = NCHCy, where Dipp = 2,6-(diisopropyl)-phenyl and Cy = cyclohexyl, which shows similar values: N. V. Kulkarni, T. Elkin, B. Tumaniskii, M. Botoshansky, L. J. W. Shimon and M. S. Eisen, *Organometallics*, 2014, **33**, 3119.

23 B. N. Figgis and J. Lewis in *Progr. Inorg. Chem.*, ed. F. A. Cotton, WileyWiley, New York, 1964, vol. 6, pp.37–239.

24 $[NiCl_2(PPh_3)_2]$, (*a*) μ = 3.07 μ_B: L. M. Venanzi, *J. Chem. Soc.*, 1958, 719; (*b*) μ = 3.39 μ_B at 273 K: F. A. Cotton, O. D. Faut and D. M. L. Goodgame, *J. Am. Chem. Soc.*, 1961, **83**, 344.

25 U. Casellato, D. Ajó, G. Valle, B. Corain, B. Longato and R. Graziani, *J. Crystallogr. Spectrosc. Res.*, 1988, **18**, 583(data at room temperature).

26 D. I. Arnold, F. A. Cotton, D. J. Maloney, J. H. Matonic and C. A. Murillo, *Polyhedron*, 1997, **16**, 133 (data at −60 °C).

27 L. Yang, D. R. Powell and R. P. Houser, *Dalton Trans.*, 2007, 955.

28 Despite the distortion, the {N1,P1,N1} and {Ni1,Cl1,Cl2} planes remain close to perpendicular (88.57(6)°). The dihedral angles between the {Ni1,Cl1,Cl2} plane and the planes of the cyclopentadienyl rings are 13.09(9)° for C(1–5), and 14.90(8)° for C(6–10).

29 (*a*) T. G. Appleton, H. C. Clark and L. E. Manzer, *Coord. Chem. Rev.*, 1973, **10**, 335; (*b*) F. R. Hartley, *Chem. Soc. Rev.*, 1973, **2**, 163.

30 R. G. Pearson, *Inorg. Chem.*, 1973, **12**, 712.

31 S. I. Kirin, H.-B. Kraatz and N. Metzler-Nolte, *Chem. Soc. Rev.*, 2006, **35**, 348.

32 (*a*) B. N. Storhoff and H. C. Lewis, *Coord. Chem. Rev.*, 1977, **23**, 1; (*b*) S. F. Rach and F. E. Kühn, *Chem. Rev.*, 2009, **109**, 2061.

33 K. M. Gramigna, J. V. Oria, C. L. Mandell, M. A. Tiedemann, W. G. Dougherty, N. A. Piro, W. S. Kassel, B. C. Chan, P. L. Diaconescu and C. Nataro, *Organometallics*, 2013, **32**, 5966.

34 S. Dey, F. Roesler, C. Bruhn, Z. Kelemen and R. Pietschnig, *Inorg. Chem. Front.*, 2023, **10**, 3828.

35 (*a*) K. J. Cavell, D. J. Stufkens and K. Vrieze, *Inorg. Chim. Acta*, 1981, **47**, 67; (*b*) F. Horký, I. Císařová and P. Štěpnička, *ChemCatChem*, 2021, **13**, 4848; (*c*) F. Horký, J. Schulz, M. Zábranský and P. Štěpnička, *Eur. J. Inorg. Chem.*, 2023, e202300126.

36 For examples of [Pd(L^L)(ma)] complexes with unsymmetric chelating ligands L^L, see: (*a*) K. Selvakumar, M. Valentini, P. S. Pregosin and A. Albinati, *Organometallics*, 1999, **18**, 4591; (*b*) J.-Y. Lee, J.-S. Shen, R.-J. Tzeng, I.-C. Lu, J.-H. Lii, C.-H. Hu and H. M. Lee, *Dalton Trans.*, 2016, **45**, 10375; (*c*) J. Huang, T. Keenan, F. Richard, J. Lu, S. E. Jenny, A. Jean, S. Arseniyadis and D. C. Leitch, *Nat. Commun.*, 2023, **14**, 8058.

37 (*a*) M. J. S. Dewar, *Bull. Soc. Chem. Fr.*, 1951, **18**, C71; (*b*) J. Chatt and L. A. Duncanson, *J. Chem. Soc.*, 1953, 2939.

38 M. Lutz, *Acta Crystallogr., Sect. E: Struct. Rep. Online*, 2001, **57**, o1136.

39 The barrier of internal rotation of the cyclopentadienyl rings determined for unsubstituted ferrocene was only 4 kJ mol^{-1}: A. Haaland and J. E. Nilsson, *Chem. Commun.*, 1968, 88.

40 J. C. Green, *Coord. Chem. Rev.*, 1998, **27**, 263.

41 R. E. Rülke, J. M. Ernsting, A. L. Spek, C. J. Elsevier, P. W. N. M. van Leeuwen and K. Vrieze, *Inorg. Chem.*, 1993, **32**, 5769.

42 Z. Leitner, I. Císařová, J. Kalbáčová Vejpravová and P. Štěpnička, CCDC 2469284: Experimental Crystal Structure Determination, 2025, DOI: **10.5517/ccdc.csd.cc2nwhbd**.

43 Z. Leitner, I. Císařová, J. Kalbáčová Vejpravová and P. Štěpnička, CCDC 2469285: Experimental Crystal Structure Determination, 2025, DOI: **10.5517/ccdc.csd.cc2nwhcf**.

44 Z. Leitner, I. Císařová, J. Kalbáčová Vejpravová and P. Štěpnička, CCDC 2469286: Experimental Crystal Structure Determination, 2025, DOI: **10.5517/ccdc.csd.cc2nwhdg**.

45 Z. Leitner, I. Císařová, J. Kalbáčová Vejpravová, P. Štěpnička, CCDC 2469287: Experimental Crystal Structure Determination, 2025, DOI: **10.5517/ccdc.csd.cc2nwhfh**.

46 Z. Leitner, I. Císařová, J. Kalbáčová Vejpravová and P. Štěpnička, CCDC 2469288: Experimental Crystal Structure Determination, 2025, DOI: **10.5517/ccdc.csd.cc2nwhgj**.

47 Z. Leitner, I. Císařová, J. Kalbáčová Vejpravová and P. Štěpnička, CCDC 2469289: Experimental Crystal Structure Determination, 2025, DOI: **10.5517/ccdc.csd.cc2nwhhk**.

48 Z. Leitner, I. Císařová, J. Kalbáčová Vejpravová and P. Štěpnička, CCDC 2469290: Experimental Crystal Structure Determination, 2025, DOI: 10.5517/ccdc.csd.cc2nwhjl.
49 Z. Leitner, I. Císařová, J. Kalbáčová Vejpravová and P. Štěpnička, CCDC 2469291: Experimental Crystal Structure Determination, 2025, DOI: 10.5517/ccdc.csd.cc2nwhkm.
50 Z. Leitner, I. Císařová, J. Kalbáčová Vejpravová and P. Štěpnička, CCDC 2469292: Experimental Crystal Structure Determination, 2025, DOI: 10.5517/ccdc.csd.cc2nwhln.
51 Z. Leitner, I. Císařová, J. Kalbáčová Vejpravová and P. Štěpnička, CCDC 2469293: Experimental Crystal Structure Determination, 2025, DOI: 10.5517/ccdc.csd.cc2nwhmp.